

Grafting Polymer Brushes on Graphene Oxide for Controlling Surface Charge States and Templated Synthesis of Metal Nanoparticles

Tingting Gao,^{1,2} Qian Ye,¹ Xiaowei Pei,¹ Yanqiu Xia,¹ Feng Zhou¹

¹State Key Laboratory of Solid Lubrication, Lanzhou Institute of Chemical Physics, Chinese Academy of Sciences, Lanzhou 730000, People's Republic of China

²Graduate University of the Chinese Academy of Sciences, Beijing 100049, People's Republic of China

Correspondence to: X. Pei (E-mail: peixw@licp.cas.cn) or Y. Xia (E-mail: xiayanqiu@yahoo.com) or F. Zhou (E-mail: zhouf@lzb.ac.cn)

ABSTRACT: In this article, poly[(dimethylamino)ethyl methacrylate] (PDMAEMA) brushes were grafted onto graphene oxide (GO) sheet via noncovalent modification of pyrene terminated initiator and subsequent *in situ* surface-initiated atom transfer radical polymerization (SI-ATRP). The results of zeta-potentials, dispersivity measurement as well as the permeability of cationic and anionic redox-active probe molecules reveal that the as-prepared GO/PDMAEMA composite exhibits zwitterionicity because of the presence of phenol hydroxyl, carboxyl, and amine groups and the charging state can be manipulated by controlling pH values. Furthermore, by ion exchange and *in situ* reduction, palladium and gold nanoparticles were successfully uploaded and the catalytic property of the uniformly distributed Pd-Au nanoparticles on GO sheet was investigated. These results reported in this work may open primarily toward constructing a bridge among GO, charged polymer and metal nanoparticles and secondarily to represent a new strategy for uniformly depositing inorganic nanoparticles.

KEYWORDS: graphene oxide; atom transfer radical polymerization; zwitterionicity; nanoparticles; stimuli-responsive polymers

Received 10 December 2011; accepted 27 February 2012; published online 00 Month 2012

DOI: 10.1002/app.37572

INTRODUCTION

Graphene oxide (GO), with intrinsic sp² networks¹ and abundant oxygen-containing groups² on its platelet and edge, has attracted worldwide attention because of its potential applications in sensors,³ energy-related materials,⁴ catalyst,⁵ drug delivery,⁶ and reinforcement filler.⁷ Functionalization of GO is expected to play a vital role in tailoring the structure and properties of GO, improving the solubility and optical⁸ properties of GO, and preparing novel GO-based nanocomposites. For example, the α -Fe₂O₃ nanorods/GO composites added in the base oil as additives showed better friction and wear properties than pure GO nanosheets in the oil.⁹ Therefore, many research groups have focused on functionalizing GO with various organic and organometallic structures and linear polymers to enhance their properties.

Among the functionalization of GO, covalent modification recently attracted considerable attention because it endows the surface with novel structure and properties.^{10–13} However, this strategy usually damages the original structure of GO sheet, and the oxygen-containing groups will be partly or totally disappeared, which results in the change of original properties of GO. Therefore, a number of research groups have focused on the non-

covalent modification of GO through noncovalent interactions such as hydrogen bond,¹⁴ electrostatic interactions,¹⁵ and van der Waals⁶ interactions. Previous studies^{16–18} indicate that pyrene derivatives,¹⁹ which have long been used to modify the carbon nanotube via π - π stacking, can successfully functionalize the GO and graphene sheet. For example, Shi and coworkers¹⁶ firstly reported the noncovalent functionalization of GO sheets via π - π stacking using 1-pyrenebutyrate, followed by *in situ* reduction to prepare stable aqueous dispersions of graphene sheets. With noncovalent interactions, hydroxyl, carboxyl, and epoxy groups on GO sheet and the intrinsic properties associated with these groups were preserved. Thus, the negative charged and pH responsive properties of the GO sheet resulted from these oxygen-containing groups can be successfully studied in this article.

Stimuli-responsive polymers can construct a “smart” surface due to their conformation and structure change in response to a variety of external stimuli^{20–23} such as solvent, temperature, pH, ions, light, etc. Such “smart” polymers have potential applications in gates to control the permeability in surface coatings in chromatographic separations, controlled release systems, and actuation devices.^{24–26} The weak polyelectrolyte brush with

charge density strongly depending on solution pH has already attracted intense attention.^{27,28} The polyelectrolyte brush with zwitterionicity, which exhibits reversible, pH-switchable permselectivity for both cations and anions is highly desired to construct a more intelligent surface.^{29,30} Recently, some pH-sensitive graphene or GO based materials have been prepared by modifying them with pH responsive polymers^{17,31,32} such as PDMAEA, PAA, PAM, and Lysozyme via covalent or noncovalent interactions. However, these studies mainly focused on the pH responsive properties of the polymer chains, little attention has been paid to intrinsic pH responsive properties of GO resulted from these active oxygen groups. Wallace and co-workers³³ indicated that the GO sheet was negatively charged in aqueous by zeta-potential analysis and the charge density changes with different pH values, enabling the GO sheet to be pH responsive. Ishida and coworkers have³⁴ obtained the metal-metal oxide nanoparticles decorated graphene sheets from ion-exchanged GOs, which indicate that the GO has the potential for selective permeability towards counterions. Studies^{29,30,35} on polymer brushes containing amine groups, phenol hydroxyl, or carboxyl groups on its chains demonstrates their ionic permselectivity at different pH values. As a common pH responsive polymer, which containing amine groups, PDMAEMA can be grafted onto GO sheets via π - π stacking and the coexistence of amine, phenol hydroxyl, and carboxyl functional groups is anticipated to make the composite amphiprotic. It is well known that the inorganic nanoparticles, such as Pd, Au, Pt, etc., with excellent electronic, optical, and catalytic performance have been widely studied.^{36,37} And these nanoparticles can be template synthesized via the ion exchange of the polyelectrolyte counterions and *in situ* preparation method with the controlled size and uniform distribution.³⁸ Relatively, the zwitterionicity of the GO/PDMAEMA composite may be used for exchange with both cationic and anionic ions to prepare two different nanoparticles on the composite.

In this article, we prepared the initiator modified GO through noncovalent π - π interaction followed by ATRP polymerization to afford the GO/PDMAEMA composite. Zeta-potentials, dispersivity measurement as well as the permeability of cationic and anionic redox-active probe molecules, were used to evaluate the zwitterionicity of the as-prepared GO/PDMAEMA composite. As prove of concept, by using zwitterionicity of GO/PDMAEMA composite, Pd-Au nanoparticles were controlled and uniformly uploaded via cations and anions exchange followed *in situ* reduction method, with the aim of integrating the excellent catalytic properties of noble metal nanoparticles^{36,37} and good supporting behavior of graphene or GO based materials for loading nanoparticles.¹

EXPERIMENTAL

Materials

Monomer 2-(dimethylamino) ethyl methacrylate, 1-pyrenebutanol were purchased from Aldrich and were used as received without further purification. Copper(I) bromide was purified by reflux in acetic acid. Sodium methacrylate (MAA-Na), $K_3Fe(CN)_6$, $K_4Fe(CN)_6$, $Ru(NH_3)_6Cl_3$, $HAuCl_4$, $Pd(NH_3)_4Cl_2$, 2-Bromoisobutryl bromide, graphite (powered flake graphite)

were obtained from Alfa Aesar. Ultrapure water used throughout the experiments was obtained from a NANOpure Infinity system from Barnstead/Thermolyne Corp. Other reagents were used as received.

Synthesis of the Initiator

Into a dried flask, 1-pyrenebutanol (274.4 mg, 1 mmol), triethylamine (0.7 mL, 5 mmol), and 10 mL of anhydrous dichloromethane (CH_2Cl_2) were charged. The solution was continuously stirred at 0°C, and 2-Bromoisobutryl bromide (0.25 mL, 2 mmol) was added dropwise via a syringe. The reaction mixture was stirred at room temperature for 2 h, and then extracted with CH_2Cl_2 (3×100 mL). The combined organic phase was dried over anhydrous $MgSO_4$, and the solvent was evaporated under reduced pressure. The crude product was purified by using silica gel column chromatography (10% MeOH in $CHCl_3$) to give a white solid (0.34 g, yield 80%, mp 60–63°C).

¹H-NMR (400 MHz, $CDCl_3$ TMS), δ (ppm): 8.25 (d, $J = 9.2$ Hz, 1H), 7.96–8.16 (m, 7H, CH_{arom}), 7.85 (d, $J = 8.0$ Hz, 1H), 4.25 (t, $J = 6.4$ Hz, 2H), 3.38 (t, $J = 7.6$ Hz, 2H), 1.93–2.01 (m, 2H), 1.91(s, 6H), 1.84–1.88 (m, 2H).

¹³C-NMR (100 MHz, $CDCl_3$ TMS), δ (ppm): 171.7, 136.2, 131.4, 130.9, 129.9, 128.6, 127.5, 127.3, 127.2, 126.6, 125.8, 125.1, 125.0, 124.9, 124.8, 124.7, 123.3, 65.8, 55.9, 33.0, 30.8, 28.4, 28.0.

Preparation of the Initiator Modified Graphene Oxide

GO was prepared by oxidation of flake graphite using $KMnO_4/H_2SO_4/NaNO_3$ according to a modified Hummers' method.³⁹ Typically, GO (100 mg) was dispersed in a 0.08 mM acetone solution of initiator, after sonication for 30 min, the mixture was stirred at room temperature for 24 h. Then the initiator modified GO were carefully separated and purified by repeated washing with acetone using centrifugation.

Preparation of GO-g-PDMAEMA Nanocomposite via Surface-Initiated ATRP Polymerization

Typically, 2 mL DMAEMA monomer and 20 mL 1 : 1 (v : v) MeOH/ H_2O mixture were charged into a flask under Ar flow for 20 min, then 120.0 mg bipyridyl and 60.8 mg CuBr were added quickly and purged again with Ar flow for 20 min. The polymerization was started at room temperature under Ar protection immediately after the addition of 20 mg initiator modified GO. After 2 h, the PDMAEMA modified GO (denoted as GO-g-PDMAEMA) were separated from the reaction medium and thoroughly washed with ultrapure water and ethanol using centrifugation. The samples were further dried under vacuum overnight before further analysis. The PMAA-Na modified GO (denoted as GO-g-PMAA-Na) was prepared in the same way.

Deposition of Pd Nanoparticles on GO-g-PDMAEMA Composite

The GO-g-PDMAEMA composite was dispersed in pH = 11 solution for 2 h, and washed with pure water using centrifugation. The resulting product was then immersed in 0.1M $Pd(NH_3)_4Cl_2$ aqueous solution for 1 h to exchange cations, and subsequently immersed in a fresh 0.1M $NaBH_4$ solution for 30 min to afford the Pd nanoparticles which were uniformly loaded on GO-g-

PDMAEMA composite (the product noted as GO-g-PDMAEMA/Pd(0) nanocomposite).

Preparation of Pd-Au Bimetallic Nanoparticles on GO-g-PDMAEMA/Pd(0) Nanocomposite

Firstly, quaternization of PDMAEMA chains was carried out in iodomethane/CH₃NO₂ (1 : 5) at room temperature for 24 h to afford a GO-Q-PDMAEMA/Pd(0) composite. Then the GO-Q-PDMAEMA/Pd(0) nanocomposite was dispersed in 50 mM HAuCl₄ solution for 1 h to exchange anions, and subsequently reduced with 0.1M NaBH₄ solution to obtain the GO-Q-PDMAEMA/Pd(0)-Au(0) nanocomposite. The nanocomposite was separated and purified by repeated washing with water.

Preparation of GO Nanocomposites/ITO Electrode

The GO/ITO, GO-g-PMAA-Na/ITO and GO-g-PDMAEMA/ITO electrodes were prepared as follows: 10 mg samples, 2 mL ethanol, 0.5 mL 0.5% PEG-2000 [Poly(ethylene glycol)] ethanol solution, 0.02 mL OP emulsifier, and 0.04 mL acetylacetone were added into an agate mortar and grinded for 1 h, the obtained solution was applied by a micropipet to the ITO electrode surface.

Catalytic Reduction of 4-Nitrophenol

Firstly, 0.5 mL of sodium borohydride (1.2 mg) aqueous solution was added to 2.5 mL of 4-nitrophenol (0.042 mg) aqueous solution contained in a quartz cuvette.⁴⁰ After that, a given amount of GO-Q-PDMAEMA/Pd(0)-Au(0) nanocomposite was added immediately. UV spectra of the solution were taken at regular intervals in the range of 250–550 nm. The rate constant of the reaction was determined by measuring the change in intensity of the initially observed peak at 400 nm with time.

Characterization

¹H-NMR and ¹³C-NMR spectra were recorded on a 400 MHz spectrometer (Bruker AM-400) using CDCl₃ as the solvent. AFM image was taken by using a multimode AFM (Nanoscope IIIa, Veeco Instrument, Santa Barbara, CA) operating in the tapping mode. Attenuated total reflection infrared (ATR-IR) spectra were recorded on a Nicolet is10 instrument (Thermo Nicolet Corporation). Thermal stability was determined with a thermogravimetric analyzer (TGA) (Perkin-Elmer, PET) over a temperature range of 25–800°C at a heating rate of 10°C/min under N₂ atmosphere. Zeta-potential of the samples was measured by Malvern Zetasizer Nano ZS ZEN 3600 in different pH solutions. Electrochemical experiments were performed at room temperature using a CHI 660B electrochemical workstation (Shanghai, China). A conventional three-electrode cell was used, including a saturated calomel electrode (SCE) as reference electrode, a platinum counter electrode, and modified ITO electrode as working electrode. Chemical composition information of the samples was obtained by X-ray photoelectron spectroscopy (XPS); the measurement was carried out on a PHI-5702 multifunctional spectrometer using Al K- α radiation, and the binding energies were referenced to the C1s line at 284.8 eV from adventitious carbon. The morphology was investigated by transmission electron microscopy (TEM) (Hitachi Model JEM-2010). The UV–vis absorption spectra were recorded on a UV–visible spectrophotometer (Hewlett-Packard 8453A) every 15 min in the range 250–550 nm at 12°C.

RESULTS AND DISCUSSION

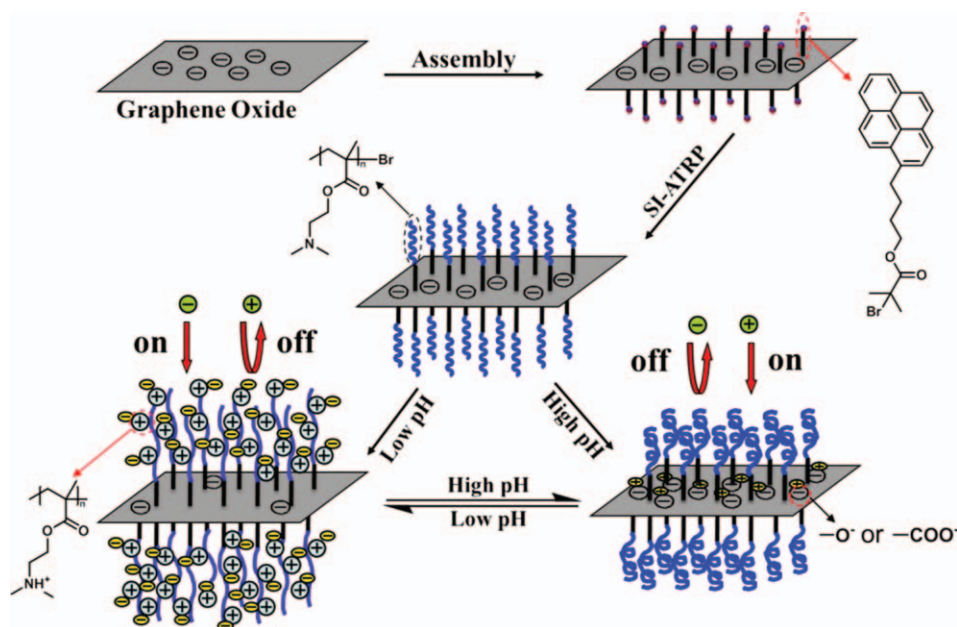
In this article, a pyrene-terminated initiator was attached on both sides of the GO surface via π – π stacking interaction. PDMAEMA chains were subsequently grafted from the surface of sheet via *in situ* ATRP polymerization of DMAEMA to produce the GO-g-PDMAEMA composite. Scheme 1 shows the detailed approach to grow polymer brushes onto GO sheet and charging state of the GO-g-PDMAEMA composite at different pH values.

Preparation and Characterization of GO-g-PDMAEMA and GO-g-PMAA-Na Composite

The atomic force microscopic (AFM) images of unmodified GO sheet and GO-g-PDMAEMA composite were shown in Figure 1. The samples were prepared by depositing GO dispersion in water and GO-g-PDMAEMA in basic solution onto a silicon wafer, respectively and dried under N₂ flow. Because of the adsorbed water⁴¹ and the oxygen groups⁴² on both sides of single GO sheet, the GO sheets are expected to be much thicker than the pristine graphene sheets \sim 0.34 nm.⁴³ The cross-sectional view of the typical AFM image of the exfoliated GO in Figure 1(a) displays that the average thickness of the monolayer GO is \sim 1.2 nm, similar to earlier studies.^{43,44} This indicates the full exfoliation of graphite oxide. After the surface modification of GO with PDMAEMA, the AFM analysis [Figure 2(b)] reveals that the thickness of the “sandwich” composite is \sim 4.2 nm, much thicker than the original GO sheet.

The ATR-IR spectra were employed to further confirm the polymer coatings. For the original GO sheet, as shown in Figure 2(a), a wide band at 3000–3700cm⁻¹ is attributed to the hydroxyl stretching vibration of the edge carboxyl groups and basal plane hydroxyls on GO sheets as well as the adsorbed water⁴¹; the band at 1735 and 1690 cm⁻¹ are attributed to the C=O stretch of the carboxyl and/or carbonyl group on GO sheet⁴¹ and the peak at 1607cm⁻¹ is attributed to aromatic C=C double bond stretching vibration.⁴⁵ Figure 2(b) shows the IR spectrum of the GO-g-PDMAEMA composite. Typical features of the PDMAEMA backbone include absorptions at 2951cm⁻¹ due to C–H symmetric and asymmetric stretching of methyl and –CH₂– groups, spectroscopic characteristics at 2833 and 2768 cm⁻¹ from C–H stretching of the –N(CH₃)₂ groups, sharp peaks at 1724, 1446, and 1151 cm⁻¹ from C=O stretch in the ester group, –CH₂– bending and C–N stretching of –N(CH₃)₂ groups, respectively.³⁸

Thermogravimetric analysis was carried out in order to study the thermal stability and the grafting density of the composites. It was shown in Figure 3(a) that the GO sheet has a weight loss about 54% in the range between 50 and 800°C. The sharp mass loss of about 20% at round 200°C reveals that the GO is not stable. The same result has also been observed in modified GO samples, this is mainly because of the decomposition of the oxygen-containing groups and the evaporation of the intercalated water under 200°C.^{41,46} It also indicates that the oxygen groups are still on GO sheet after surface modification of PDMAEMA chains. Figure 3(c) shows a three-step degradation profile for GO-g-PDMAEMA samples. As compared with Figure 3(a,b), a graft polymer sample



Scheme 1. Schematic illustration of the preparation of PDMAEMA modified graphene oxide and charging state of the GO-g-PDMAEMA composite at different pH values. [Color figure can be viewed in the online issue, which is available at wileyonlinelibrary.com.]

typically exhibits one thermal decomposition processes at about 400°C. The residual mass percentages of GO, GO-initiator and GO-g-PDMAEMA composite calculated from the TGA data are 46, 43, and 26% at 800°C, which indicates the content of the initiator and the polymer brushes to be 3 and 20%, respectively.

To explain the characteristic of GO-g-PDMAEMA, the PMAA-Na, which has the same carboxylic group as GO, was grafted to GO surface via SI-ATRP of MAA-Na. The samples of GO and GO-g-PMAA-Na treated with different pH solutions were analyzed by ATR-IR spectra. As seen from Figure 4(a,b), when the GO sheet was treated with alkali (b), the absorptions at 1735 and 1690 cm^{-1} disappeared, while a wide peak appears at

1360–1580 cm^{-1} , which suggests that the carboxyl were converted to their basic form. The successful grafting of PMAA-Na chains on GO were substantiated by IR spectra. After modification with PMAA-Na, the adsorption peaks of the carboxyl and carbonyl groups on GO disappeared because of the presence of PMAA-Na chains. IR spectra of the GO-g-PMAA-Na [Figure 4(c)] exhibits absorption peak at 1564 cm^{-1} , which were assigned to the asymmetric vibration of the carboxylate groups⁴⁷ in GO-g-PMAA-Na. After treated with acid, the carboxylate groups were converted to protonated carboxylic group, which was confirmed by the presence of a shoulder peak at 1705 cm^{-1} corresponding to the carboxylic stretching vibration⁴⁸ [Figure 4(d)].

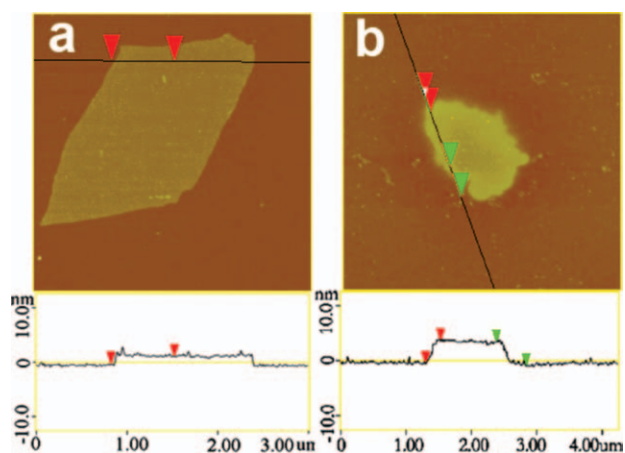


Figure 1. Typical AFM images and height profile of exfoliated graphene oxide (GO) (~ 1.2 nm) (a) and GO-g-PDMAEMA composite (~ 4.2 nm) (b) on silicon wafers. [Color figure can be viewed in the online issue, which is available at wileyonlinelibrary.com.]

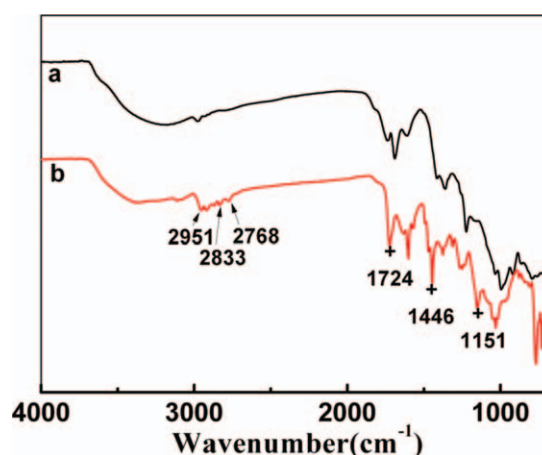


Figure 2. ATR-IR spectra of (a) GO and (b) GO-g-PDMAEMA. [Color figure can be viewed in the online issue, which is available at wileyonlinelibrary.com.]

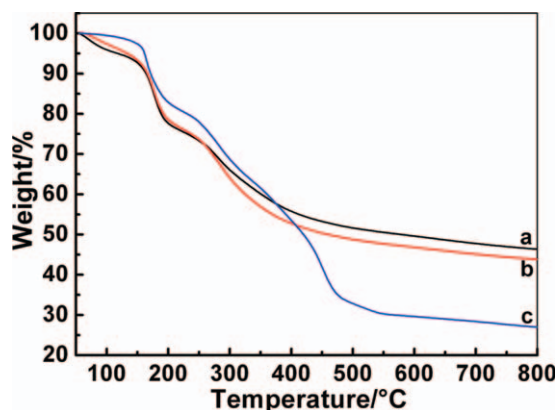


Figure 3. TGA curves of exfoliated (a) GO, (b) GO-initiator, and (c) GO-g-PDMAEMA composite. [Color figure can be viewed in the online issue, which is available at wileyonlinelibrary.com.]

Dispersing Properties and Electrochemical Properties of GO-g-PDMAEMA and GO-g-PMAA-Na Composite

GO and GO-g-PMAA-Na composite exhibit a good pH-responsive property. As shown in Figure 5, the GO and GO-g-PMAA-Na were well dispersed in alkaline aqueous media of pH 10.0 at room temperature. Their precipitation can be selectively controlled by adjusting the pH of aqueous media to 3.0. As aforementioned, the two composites have the same functional groups-hydroxyl and carboxyl groups. These groups are ionized in alkali, resulting in the negatively charged polyelectrolyte. Strong interactions can thus exist between polyelectrolyte and solvent, as well as strong electrostatic repulsion also exists within negatively charged macromolecules. These make the two composites well dispersed in alkaline conditions.^{49,50} While in an acidic environment, less negative charge exists within the composite and hydrophobic property of the polymers increased. Interactions between macromolecules are stronger than the macromolecules-solvent interactions, the composites thus grad-

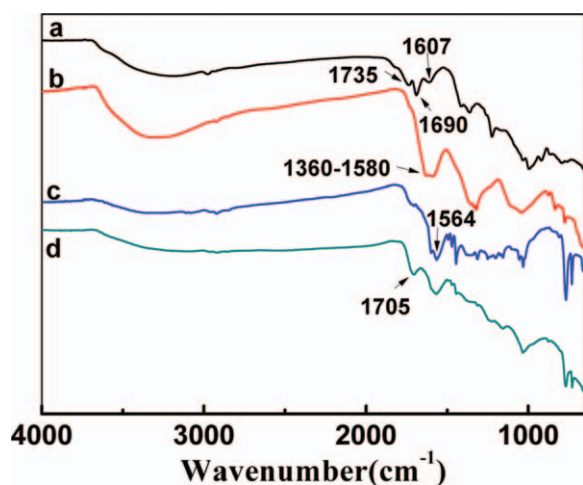


Figure 4. ATR-IR spectra of GO (a, b) and GO-g-PMAA-Na composite (c, d) at different pH values. [Color figure can be viewed in the online issue, which is available at wileyonlinelibrary.com.]

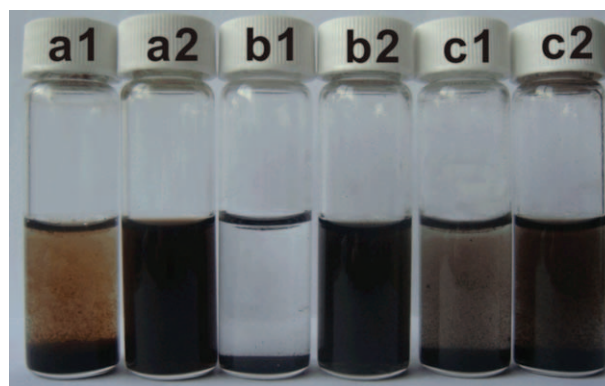


Figure 5. Photographs of GO (a1, a2), GO-g-PMAA-Na composite (b1, b2) and GO-g-PDMAEMA composite (c1, c2) in buffer solutions with different pH values. (a1, b1, c1 pH = 3.0; a2, b2, c2 pH = 10.0). [Color figure can be viewed in the online issue, which is available at wileyonlinelibrary.com.]

ually aggregated and precipitated. The PDMAEMA is also a pH-responsive polymer, but the PDMAEMA modified GO composite is not well dispersed in both acidic and basic solutions as was shown in Figure 5 (c1,c2). As we all know, PDMAEMA chains are positively charged because of the protonation of amine group in acid, thus it can be well dispersed in acid as a result of the electrostatic repulsion between the macromolecules; while in basic conditions, the PDMAEMA chains with strong hydrophobic collapsed and were not well dispersed in solution. The PDMAEMA modified GO composite contains hydroxyl, carboxyl, and amine groups simultaneously. In acidic environment the amine group made the composite dispersible in the solution while the hydroxyl and carboxyl groups made it tend to precipitate from the solution; on the contrary, in the basic condition the hydroxyl and carboxyl groups made the composite dispersible in the solution while the PDMAEMA chains facilitate its precipitation from the solution. Structure of the GO-g-PDMAEMA composite in different pH solutions was shown in Scheme 1. The presence of the two opposite roles results in the poor dispersion of GO-g-PDMAEMA composite in both conditions.

Zeta-potential is widely used for quantification of the magnitude of the electrical charge at the double layer, and its value is closely related to the stability of dispersions.³² To further prove the above theoretical analysis, zeta-potentials of GO, GO-g-PMAA-Na, GO-g-PDMAEMA in buffer solutions at different pH (3.0, 7.0, and 10.0) were measured. When the zeta-potential value is less than 15 mV, electrostatic repulsion is not sufficient to overcome the van der Waals attraction of polymer particles, the particles will gradually aggregate and precipitate from the solution.⁵¹ As seen from Table I, the zeta-potential of materials were -29.8 mV for GO and -25.7 mV for GO-g-PMAA-Na in pH 10.0 media. These materials surface thus have a lot of negative charge because its zeta-potential is higher than 20 mV. However, the zeta-potential of the GO-g-PDMAEMA is just -14.6 mV in the same buffer solutions, which means less negative charge on the materials surface. All of the three composite materials have less charge in pH 3.0 buffer solutions and the

Table I. Zeta-Potentials of GO, GO-g-PMAA-Na, GO-g-PDMAEMA in Solutions Buffered at pH 3.0, 7.0, and 10.0

Samples	Zeta-potential		
	pH = 3.0	pH = 7.0	pH = 10.0
GO	-13.6 mV	-25.1 mV	-29.8 mV
GO-PDMAEMA	13.3 mV	-3.96 mV	-14.6mV
GO-PMAA Na	-4.5 mV	-23 mV	-25.7 mV

absolute value of zeta-potential is within 15 mV. The most significant difference is that the PDMAEMA modified GO composite is positively charged, due to the protonation of amine group of PDMAEMA chains on GO, while other two composites are negatively charged. The analysis of zeta-potential is in accordance with the results observed in Figure 5.

According to the previous analysis, all the three composite prepared are pH responsive materials, i.e., charge density of the samples changes with the solution pH, the materials are anticipated to exhibit permeability toward ions in different pH conditions. The ionic permeability of GO, GO-g-PDMAEMA, and GO-g-PMAA-Na films coated ITO electrode was investigated under different pH conditions by using anionic $[\text{Fe}(\text{CN})_6]^{3-/4-}$ and cationic $[\text{Ru}(\text{NH}_3)_6]^{3+}$ as redox probe molecules. Figure 6 shows cyclic voltammograms of electrodes modified with the composite films in an aqueous solution containing 1 mM of either $[\text{Fe}(\text{CN})_6]^{3-/4-}$ or $[\text{Ru}(\text{NH}_3)_6]^{3+}$ buffered at pH 3.0, 7.0, and 10.0. The shape and magnitude of these voltammograms are significantly affected by pH. The peak current density of the GO-g-PDMAEMA films resulting from $[\text{Fe}(\text{CN})_6]^{4-}$ oxidation is about 0.7 mA/cm^2 at pH 3.0 while there is only a much small oxidation current at pH 10.0. The voltammetric results clearly

indicate that the GO-g-PDMAEMA films are open ("On") to the negatively charged probe, $[\text{Fe}(\text{CN})_6]^{3-/4-}$, at pH 3.0, but impermeable ("Off") to the probe at pH 10.0 (Scheme 1). This is resulted from the change of charge density in different pH conditions. At low pH the amino on polymer chains was protonated to make the polymer composite a positive charge, it thus attracts and passes the anions; while at high pH the phenol hydroxyl group and carboxyl groups on GO sheets were ionized, i.e., the polymer composite was negatively charged, thereby anions are repulsed and resulting a small current. When using the positively charged $[\text{Ru}(\text{NH}_3)_6]^{3+}$ as probe, the "On/Off" behavior of the GO-g-PDMAEMA composite films reversed, the peak current density is large at high pH (10.0) and small at low pH (3.0). However, the value and change of the peak current density in different pH are much smaller than the negatively charged probe, so that the "on/off" function for $[\text{Ru}(\text{NH}_3)_6]^{3+}$ is not as efficient as it is for $[\text{Fe}(\text{CN})_6]^{3-/4-}$, this is due to the differences in the mass transfer rates of the two different redox probes in the film.⁵² As seen from Figure 6, though the GO and GO-g-PMAA Na composites are both pH responsive, the peak current density change with different pH values when using $[\text{Fe}(\text{CN})_6]^{3-/4-}$ or $[\text{Ru}(\text{NH}_3)_6]^{3+}$ as redox probe molecules, small change in the peak current can be observed between pH 7.0 and 10.0, even it is opposite when using $[\text{Ru}(\text{NH}_3)_6]^{3+}$ as probe. As shown in Table I, the zeta-potential of these two composites is similar between pH 7.0 and 10.0 conditions, with respect to small changes of the negative charge density, which is thought to be responsible for the result.

Electrochemical impedance spectroscopy (EIS), which is an effective method to probe the resistance properties of the polymer functionalized electrode,⁵³ was also conducted to measure the interfacial resistance in response to solution pH. Usually, a

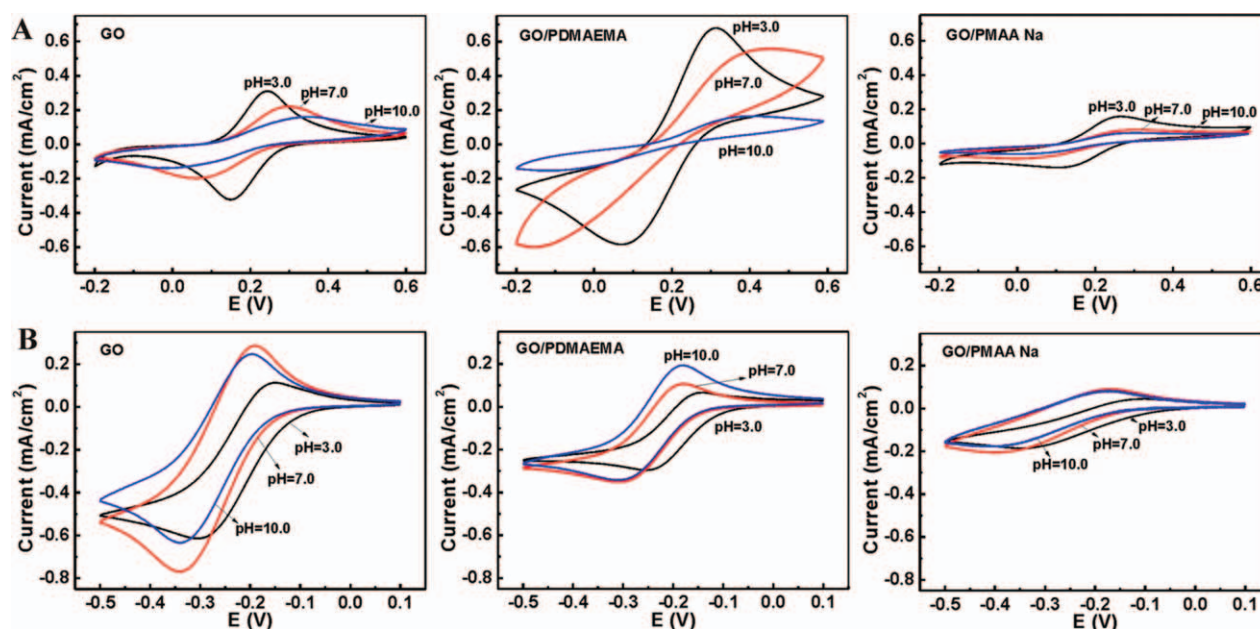


Figure 6. Cyclic voltammograms of the electrode modified by GO, GO/PDMAEMA, and GO/PMAA-Na composite in solutions containing 1 mM $[\text{Fe}(\text{CN})_6]^{3-/4-}$ (A) or $[\text{Ru}(\text{NH}_3)_6]^{3+}$ (B) buffered at pH 3.0, 7.0, and 10.0, the scan rate was 50 mV/s. [Color figure can be viewed in the online issue, which is available at wileyonlinelibrary.com.]

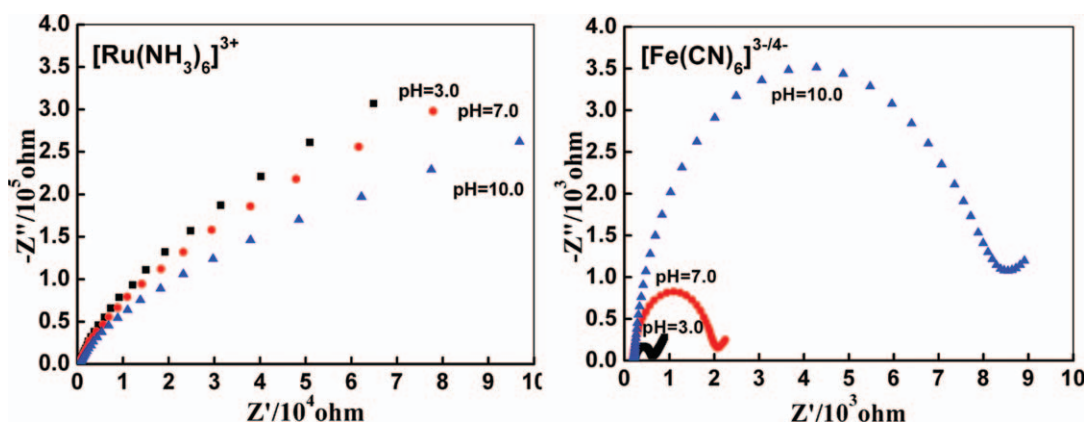


Figure 7. Nyquist plots of GO-g-PDMAEMA composite modified ITO electrode in different pH solutions using $[\text{Fe}(\text{CN})_6]^{3-/4-}$ and $[\text{Ru}(\text{NH}_3)_6]^{3+}$ as probe. [Color figure can be viewed in the online issue, which is available at wileyonlinelibrary.com.]

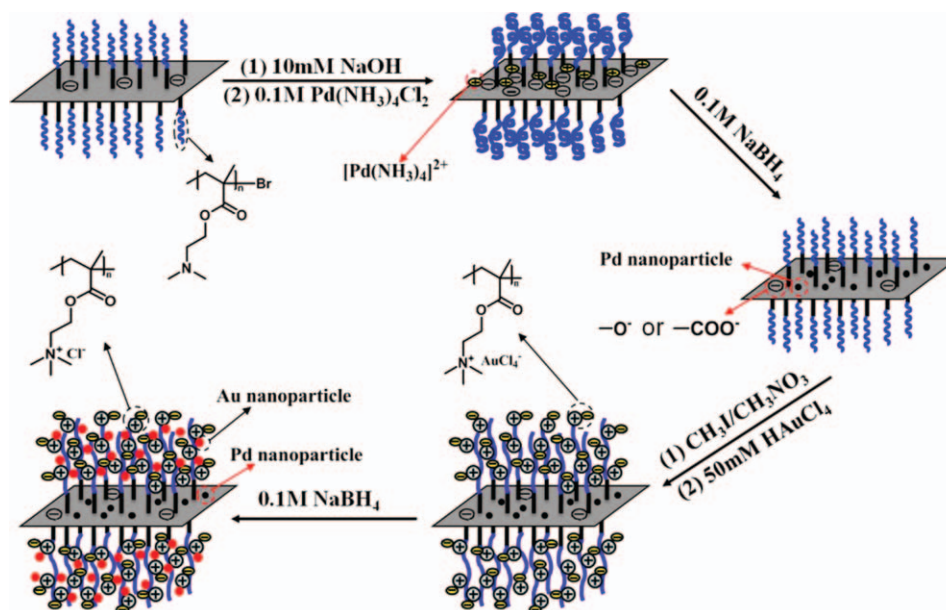
typical shape of an electrochemical impedance spectrum presents in the form of a Nyquist plot, includes a semicircle region at higher frequencies and followed by a straight line at the lower frequency. The diameter of the semicircle corresponds to the charge transfer resistance (Rct) of the probe in electron transfer, the value of which depends on the dielectric and insulating characteristics of the surface layer. Figure 7 shows the Nyquist plots of the electrode modified with GO-g-PDMAEMA composite, which was measured in different buffer solutions (pH 3.0, 7.0, and 10.0.) using $[\text{Fe}(\text{CN})_6]^{3-/4-}$ and $[\text{Ru}(\text{NH}_3)_6]^{3+}$ as probe. The results indicate that the charge transfer resistance of GO-g-PDMAEMA increases with the solution pH ranging from 3.0 to 10.0 using anionic probe and systematically decreases when using cationic probe, which is attributed to the negative charge density of the polymer increase with the pH increase. This is in accordance with the cyclic voltammograms.

The studies of cyclic voltammograms and EIS indicate that there is much difference between the GO/PDMAEMA and other two composite materials, the GO/PDMAEMA composite film can responsive to both anionic and cationic probe, while the GO and GO/PMAA-Na are not as sensitive as the GO/PDMAEMA composite, which is resulted from the positive charge induced by the PDMAEMA chains.

Preparation and Characterization of GO-g-PDMAEMA/Noble Metal Nanoparticles Composites

By using zwitterionicity of the as prepared GO-g-PDMAEMA composite, Pd-Au nanoparticles were deposited on the composite via regenerative counter ion exchange *in situ* reduction method³⁸ as depicted in Scheme 2.

Nanoparticles can be intuitively seen on GO sheet from TEM images, and XPS measurements were further conducted to



Scheme 2. Schematic illustration of the uploading noble metal nanoparticles on GO-Q-PDMAEMA composite via regenerative counterion exchange and chemical reduction. [Color figure can be viewed in the online issue, which is available at wileyonlinelibrary.com.]

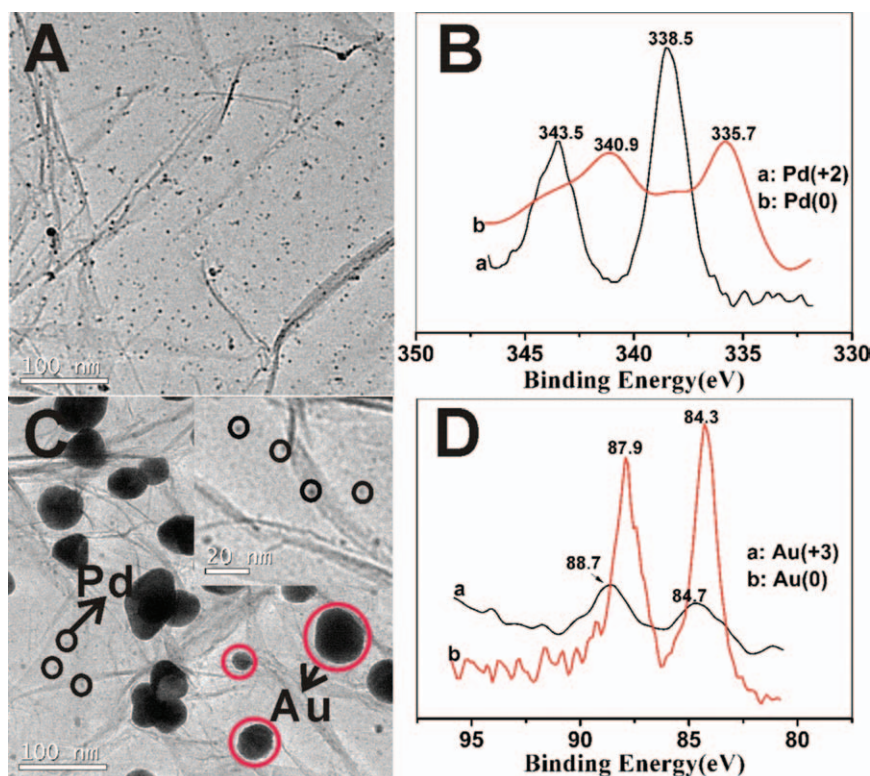


Figure 8. TEM images of GO-g-PDMAEMA/Pd(0) (A), GO-Q-PDMAEMA/Pd(0)-Au(0) (C) and the corresponding XPS spectra of GO-g-PDMAEMA/Pd(0) in the Pd(3d) (B) and GO-Q-PDMAEMA/Pd(0)-Au(0) in the Au(4f) (D) level regions before (curve a) and after (curve b) reduction. [Color figure can be viewed in the online issue, which is available at wileyonlinelibrary.com.]

confirm the chemical reduction of $[\text{Pd}(\text{NH}_3)_4]^{2+}$ and AuCl_4^- to form Pd and Au nanoparticles. From Figure 8(a), the Pd nanoparticles can be seen clearly on the GO sheet with particle size at 2–5 nm. As depicted in Figure 8(b), the Pd ($3d_{3/2}$) and Pd ($3d_{5/2}$) peaks present at 338.5 and 343.5 eV, respectively, prior to the reduction. After reduction, the peaks shift to 335.7 and 340.9 eV, this is consistent with the change in oxidation state from +2 to 0. Figure 8(c) shows TEM images of the Pd-Au nanoparticles decorated on GO sheet with Pd and Au nanoparticles are circled in black and red ring, respectively. After deposited Au nanoparticles, the Pd nanoparticles can still be seen clearly from Figure 8(c) and the insert high resolution image with the particle size not significantly changed. As contrast to the Pd nanoparticles, the Au nanoparticles appear to be much larger (15–80 nm). In Figure 7(d), the Au ($4f_{7/2}$) and Au ($4f_{5/2}$) peaks present at 84.7 and 88.7 eV assigned to Au(III). After reduction, the peaks shift to 84.3 and 87.9 eV, this suggests the formation of Au nanoparticles.

Catalytic Properties of the GO-Q-PDMAEMA/Noble Nanoparticles Composites

The catalytic properties of the composites were tested in the reduction of 4-nitrophenol by an excess of NaBH_4 .^{36,37} The reduction can be measured by the disappearance of the 400 nm peak with the concomitant appearance of a new peak at 290 nm attributable to 4-aminophenol.⁵⁴ The process of reduction was monitored by measuring change of the UV-vis absorption peak

at 400 nm at different time. Figure 9 displays the evolution of UV spectra in catalytic reduction of 4-nitrophenol by NaBH_4 . It demonstrates the catalytic performance of GO-Q-PDMAEMA/Pd(0)-Au(0) by the concentration's systematic changes of the 4-nitrophenol with the reaction time.

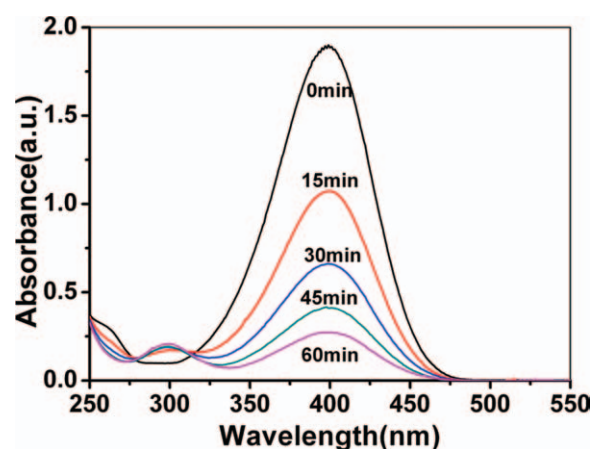


Figure 9. UV spectra for the successive reduction of 4-nitrophenol by NaBH_4 in the presence of GO-Q-PDMAEMA/Pd(0)-Au(0) with different time. The concentrations of the reactants were as follows: [4-nitrophenol] = 0.1 mmol/L, $[\text{NaBH}_4]$ = 10 mmol/L, catalysts = 9.5 mg/L, $T = 12^\circ\text{C}$. [Color figure can be viewed in the online issue, which is available at wileyonlinelibrary.com.]

CONCLUSIONS

Summing up, we have prepared the GO/polymer brushes composite by noncovalent π - π interaction and *in situ* ATRP polymerization. By grafting charged polymers, the surface charge states can be manipulated and controlled by pH. Through grafting positively charged polymer brushes, GO, natively negatively charged, exhibited zwitterionicity, which could be used for governing the permeability of cationic and anionic redox-active probe molecules and could be used for templated synthesis of metal nanoparticles after exchanging precursors via ionic exchange and *in situ* reduction. Hopefully, the strategy can be extended to prepare a variety of composites of GO, polymer, and inorganic nanoparticles.

ACKNOWLEDGMENTS

The work is financially supported by Key Project of NSFC (20973188, 21125316) and "Top Hundred Talents" Program of CAS.

REFERENCES

- Kamat, P. V.; Muszynski, R.; Seger, B. *J Phys Chem C* **2008**, *112*, 5263.
- Szabo, T.; Tombacz, E.; Illes, E.; Dekany, I. *Carbon* **2006**, *44*, 537.
- Chen, X.; Chen, X. M.; Wu, G. H.; Chen, J. M.; Jiang, Y. Q.; Chen, G. N.; Oyama, M.; Wang, X. R. *Biosens Bioelectron* **2010**, *26*, 872.
- Wang, L.; Lee, K.; Sun, Y.-Y.; Lucking, M.; Chen, Z.; Zhao, J. J.; Zhang, S. B. *ACS Nano* **2009**, *3*, 2995.
- Dreyer, D. R.; Jia, H.-P.; Bielawski, C. W. *Angew Chem* **2010**, *122*, 6965.
- Dai, H. J.; Liu, Z.; Robinson, J. T.; Sun, X. M. *J Am Chem Soc* **2008**, *130*, 10876.
- Putz, K. W.; Compton, O. C.; Palmeri, M. J.; Nguyen, S. T.; Brinson, L. C. *Adv Funct Mater* **2010**, *20*, 3322.
- Chen, P.; Yin, Z.; Huang, X.; Wu, S.; Liedberg, B.; Zhang, H. *J Phys Chem C* **2011**, doi: 10.1021/jp208486m.
- Song, H.-J.; Jia, X.-H.; Li, N.; Yang, X.-F.; Tang, H. *J Mater Chem* **2012**, doi: 10.1039/C1JM13740A.
- Bielawski, C. W.; Dreyer, D. R.; Park, S.; Ruoff, R. S. *Chem Soc Rev* **2010**, *39*, 228.
- Ruoff, R. S.; Park, S.; Dikin, D. A.; Nguyen, S. T. *J Phys Chem C* **2009**, *113*, 15801.
- Yang, Y. F.; Wang, J.; Zhang, J.; Liu, J. C.; Yang, X. L.; Zhao, H. Y. *Langmuir* **2009**, *25*, 11808.
- Zhang, B.; Chen, Y.; Zhuang, X.; Liu, G.; Yu, B.; Kang, E.-T.; Zhu, J.; Li, Y. *J Polym Sci A: Polym Chem* **2010**, *48*, 2642.
- Shi, G. Q.; Xu, Y. X.; Hong, W. J.; Bai, H.; Li, C. *Carbon* **2009**, *47*, 3538.
- Suh, K. S.; Kim, T.; Lee, H.; Kim, J. *ACS Nano* **2010**, *4*, 1612.
- Li, C.; Xu, Y. X.; Bai, H.; Lu, G. W.; Shi, G. Q. *J Am Chem Soc* **2008**, *130*, 5856.
- Davis, T. P.; Liu, J. Q.; Tao, L.; Yang, W. R.; Li, D.; Boyer, C.; Wuhler, R.; Braet, F. *Langmuir* **2010**, *26*, 10068.
- Davis, T. P.; Liu, J. Q.; Yang, W. R.; Tao, L.; Li, D.; Boyer, C. *J Polym Sci A: Polym Chem* **2010**, *48*, 425.
- Nakashima, N.; Tomonari, Y.; Murakami, H. *Chem Lett* **2002**, *31*, 638.
- Zhou, F.; Hu, H.; Yu, B.; Osborne, V. L.; Huck, W. T. S.; Liu, W. *Anal Chem* **2006**, *79*, 176.
- Theato, P.; Jochum, F. D.; zur Borg, L.; Roth, P. J. *Macromolecules* **2009**, *42*, 7854.
- Zhou, F.; Biesheuvel, P. M.; Chol, E. Y.; Shu, W.; Poetes, R.; Steiner, U.; Huck, W. T. S. *Nano Lett* **2008**, *8*, 725.
- Zhao, Y.-H.; Weeand, K.-H.; Bai, R. *ACS Appl Mater Interfaces* **2010**, *2*, 203.
- Liu, S. J.; Zhou, F.; Di, D. L.; Jiang, S. X. *Colloids Surf A* **2004**, *244*, 87.
- Kikuchi, A.; Okano, T. *Adv Drug Deliv Rev* **2002**, *54*, 53.
- Abu-Lail, N. I.; Kaholek, M.; LaMattina, B.; Clark, R. L.; Zauscher, S. *Sens Actuators B* **2006**, *114*, 371.
- Tran, Y.; Sanjuan, S.; Perrin, P.; Pantoustier, N. *Langmuir* **2007**, *23*, 5769.
- Zhou, F.; Huck, W. T. S. *Chem Commun* **2005**, 5999.
- Yu, B.; Liu, J.; Liu, S.; Zhou, F. *Chem Commun* **2010**, *46*, 5900.
- Liu, Y. L.; Zhao, M. Q.; Bergbreiter, D. E.; Crooks, R. M. *J Am Chem Soc* **1997**, *119*, 8720.
- Ren, L. L.; Liu, T. X.; Guo, J. A.; Guo, S. Z.; Wang, X. Y.; Wang, W. Z. *Nanotechnology* **2010**, *21*, 335701.
- Gao, L. A.; Yang, F.; Liu, Y. Q.; Sun, J. *J Phys Chem C* **2010**, *114*, 22085.
- Li, D.; Muller, M. B.; Gilje, S.; Kaner, R. B.; Wallace, G. G. *Nat Nanotechnol* **2008**, *3*, 101.
- Gotoh, K.; Kinumoto, T.; Fujii, E.; Yamamoto, A.; Hashimoto, H.; Ohkubo, T.; Itadani, A.; Kuroda, Y.; Ishida, H. *Carbon* **2011**, *49*, 1118.
- Hong, J. D.; Pennakalathil, J.; Kim, T. H.; Kim, K.; Woo, K.; Park, J. K. *Langmuir* **2010**, *26*, 11349.
- Ballauff, M.; Schrinner, M.; Talmon, Y.; Kauffmann, Y.; Thun, J.; Moller, M.; Breu, J. *Science* **2009**, *323*, 617.
- Ballauff, M.; Mei, Y.; Lu, Y.; Polzer, F.; Drechsler, M. *Chem Mater* **2007**, *19*, 1062.
- Ye, Q.; Wang, X.; Hu, H.; Wang, D.; Li, S.; Zhou, F. *J Phys Chem C* **2009**, *113*, 7677.
- Hirata, M.; Gotou, T.; Horiuchi, S.; Fujiwara, M.; Ohba, M. *Carbon* **2004**, *42*, 2929.
- Lu, Y.; Mei, Y.; Ballauff, M.; Drechsler, M. *J Phys Chem B* **2006**, *110*, 3930.
- Chabal, Y. J.; Acik, M.; Mattevi, C.; Gong, C.; Lee, G.; Cho, K.; Chhowalla, M. *ACS Nano* **2010**, *4*, 5861.
- Govindaraju, T.; Avinash, M. B.; Subrahmanyam, K. S.; Sundaraya, Y. *Nanoscale* **2010**, *2*, 1762.
- Nguyen, S. T.; Stankovich, S.; Dikin, D. A.; Piner, R. D.; Kohlhaas, K. A.; Kleinhammes, A.; Jia, Y.; Wu, Y.; Ruoff, R. S. *Carbon* **2007**, *45*, 1558.
- Huang, J. X.; Cote, L. J.; Kim, F. *J Am Chem Soc* **2009**, *131*, 1043.

45. Tour, J. M.; Marcano, D. C.; Kosynkin, D. V.; Berlin, J. M.; Sinitiskii, A.; Sun, Z. Z.; Slesarev, A.; Alemany, L. B.; Lu, W. *ACS Nano* **2010**, *4*, 4806.
46. Liu, Z. H.; Wang, Z. M.; Yang, X. J.; Ooi, K. T. *Langmuir* **2002**, *18*, 4926.
47. Park, M. K.; Deng, S. X.; Advincula, R. C. *J Am Chem Soc* **2004**, *126*, 13723.
48. Cardenas, G.; Munoz, C.; Carbacho, H. *Eur Polym J* **2000**, *36*, 1091.
49. Zharov, I.; Schepelina, O. *Langmuir* **2008**, *24*, 14188.
50. Li, Y. B.; Chen, X. D.; Zhang, M. Q.; Luo, W. A.; Yang, J.; Zhu, F. M. *Macromolecules* **2008**, *41*, 7257.
51. Herman, I. P.; White, B.; Banerjee, S.; O'Brien, S.; Turro, N. J. *J Phys Chem C* **2007**, *111*, 13684.
52. Sabatani, E.; Cohen-Boulakia, J.; Bruening, M.; Rubinstein, I. *Langmuir* **1993**, *9*, 2974.
53. Yu, B.; Zhou, F.; Hu, H.; Wang, C.; Liu, W. *Electrochim Acta* **2007**, *53*, 487.
54. Esumi, K.; Isono, R.; Yoshimura, T. *Langmuir* **2004**, *20*, 237.